Acta Crystallographica Section D
**Biological Crystallography**
ISSN 0907-4449

# Structures of two highly homologous bacterial L-asparaginases: a case of enantiomorphic space groups

**Mariusz Jaskólski,[a,b] Maciej Kozak,[a,c] Jacek Lubkowski,[d] Gottfried Palm[d]† and Alexander Wlodawer[d]***

[a]Department of Crystallography, Faculty of Chemistry, A. Mickiewicz University, Poznan, Poland, [b]Center for Biocrystallographic Research, Institute of Bioorganic Chemistry, Polish Academy of Sciences, Poznan, Poland, [c]Department of Macromolecular Physics, Faculty of Physics, A. Mickiewicz University, Poznan, Poland, and [d]Macromolecular Crystallography Laboratory, Program in Structural Biology, NCI-Frederick Cancer Research and Development Center, Frederick, MD 21702, USA

† Current address: Institute of Molecular Biotechnology, D-07708 Jena, Germany.

Correspondence e-mail: wlodawer@ncifcrf.gov



Received 14 August 2000
Accepted 12 December 2000

**PDB References:** EcA(Y25F), 1ho3; EcR(S), 1hfj; EcR(L), 1hfk.

Quasi-enantiomorphic crystals of the Y25F mutant of *Escherichia coli* L-asparaginase and of the native *Erwinia chrysanthemi* L-asparaginase were obtained in the hexagonal space groups $P6_522$ and $P6_122$, respectively. The structures of these highly homologous enzymes were solved by molecular replacement and were refined with data extending to 2.2–2.5 Å. These structures were compared with each other, as well as with other L-asparaginase structures previously observed with different crystal packing. It is concluded that the observed phenomenon, which is rare, was most likely to have arisen by chance.

## 1. Introduction

The structures of type II L-asparaginases and L-asparaginase-glutaminases from a variety of bacterial sources have been extensively characterized in the last decade. The periplasmic enzymes that belong to this family of amidohydrolases are highly homologous and several of them have been used in cancer therapy, particularly against childhood lymphoblastic leukemia (Hill *et al.*, 1967; Clavell *et al.*, 1986; Gallagher *et al.*, 1989). Refined crystal structures are currently available for enzymes isolated from *Escherichia coli* (EcA; Swain *et al.*, 1993), *Erwinia chrysanthemi* (ErA; Miller *et al.*, 1993), *Pseudomonas* 7A (PGA; Lubkowski, Wlodawer, Ammon *et al.*, 1994; Jakob *et al.*, 1997), *Acinetobacter glutaminasificans* (AGA; Lubkowski, Wlodawer, Housset *et al.*, 1994) and *Wolinella succinogenes* (WA; Lubkowski *et al.*, 1996). All of these enzymes catalyze the hydrolysis of L-asparagine to L-aspartic acid and ammonia, while some also have significant activity toward L-glutamine as a substrate. Although structural data on complexes of type II L-asparaginases with catalytic intermediates (Palm *et al.*, 1996) and inhibitors (Ortlund *et al.*, 2000) as well as extensive biochemical and mutation data (Harms *et al.*, 1991; Derst *et al.*, 1992; Wehner *et al.*, 1992; Derst *et al.*, 1994) have shed some insight on the catalytic mechanism of these enzymes, their exact mode of action is still not fully understood. In addition to these periplasmic enzymes, bacteria such as *E. coli* also produce cytosolic (or type I) asparaginases which, in spite of their sequence similarity to the type II enzymes, do not have antileukemic properties, probably because of lower substrate affinity (Beacham & Jennings, 1990).

The subunit of all well characterized type II L-asparaginases (Fig. 1) consists of a single polypeptide chain of ∼330 amino acids organized in two domains. The sequences of enzymes from different sources are highly homologous; for example, those of EcA and ErA are 46% identical (Fig. 1). The N-terminal domain (residues 1–190 according to EcA

numbering, used throughout the text unless explicitly indicated to the contrary) contains an eight-stranded mixed $\beta$-sheet flanked by four $\alpha$-helices. The smaller C-terminal domain (residues 213–326) contains a four-stranded parallel $\beta$-sheet, also flanked by four $\alpha$-helices. The two domains are connected by a structurally well defined linker. The active site, marked in the structure of EcA by a bound L-aspartate (Swain *et al.*, 1993), includes Thr12, Thr89, Gln59, Asp90, Ser58, Lys162, Asn248, Glu283 and Tyr25. The latter residue, although important for catalytic activity, is located on a flexible loop (residues ∼15–30) that is partially or completely disordered in most published structures of L-asparaginases (Lubkowski *et al.*, 1996) and serves as a mobile gate for the active site.

All known type II L-asparaginases are active as homotetramers of molecular mass ∼140 kDa arranged as 222-symmetric assemblies around three mutually perpendicular dyads (Greenquist & Wriston, 1972; Swain *et al.*, 1993). According to the nomenclature established for the first L-asparaginase structure (Swain *et al.*, 1993; Protein Data Bank code 3eca), the four subunits are labeled *A*, *B*, *C* and *D*. The closest interactions exist between the *A* and *C* subunits (as well as between the *B* and *D*), leading to the formation of two intimate dimers within which the four non-allosteric catalytic centers are created. Besides the Thr89-Lys162-Asp90 catalytic triad, reminiscent of the Ser-His-Asp active site of serine proteases (Dodson & Wlodawer, 1998), most of the other essential residues from the active site are contributed by the N-terminal domain of one subunit (for example *C*), while another subunit (in this case *A*) provides in its C-terminal domain two other essential amino acids, Asn248 and Glu283. Although the other subunits (here *B* and *D*) do not contribute to the formation of the active sites within an intimate dimer, the formation of tetramers, for reasons that are not completely clear, appears to be essential for the catalytic competence of type II enzymes. The complete homotetramers are generated through the action of the remaining two dyads. Of the two types of pairs thus formed (*AB* and *AD*, and analogously *BC* and *CD*), the *AB* pair is tighter and has a recognizable sequence and interaction pattern which is different for type II and type I L-asparaginases and may indeed be a distinguishing feature between them (Bonthron & Jaskólski, 1997).

Several crystal forms of bacterial L-asparaginases have been reported, with the contents of the asymmetric unit comprising as little as one monomer (Lubkowski, Wlodwer, Housset *et al.*, 1994) or as many as two tetrameric molecules (G. Palm, unpublished data). Multiple crystal forms are common even for the same enzyme, depending on the details of the crystallization experiments. In our attempts to further characterize L-asparaginases from different sources, we found ErA and EcA crystals that appeared to be almost isomorphous. However, detailed crystallographic analyses of the respective structures indicated that these crystals belong to two enantiomorphic space groups rather than being truly isomorphous and that their crystal packing is quite different. These observations made us question whether similar phenomena had been observed previously for other systems and whether the quasi-isomorphism could be explained on structural grounds.

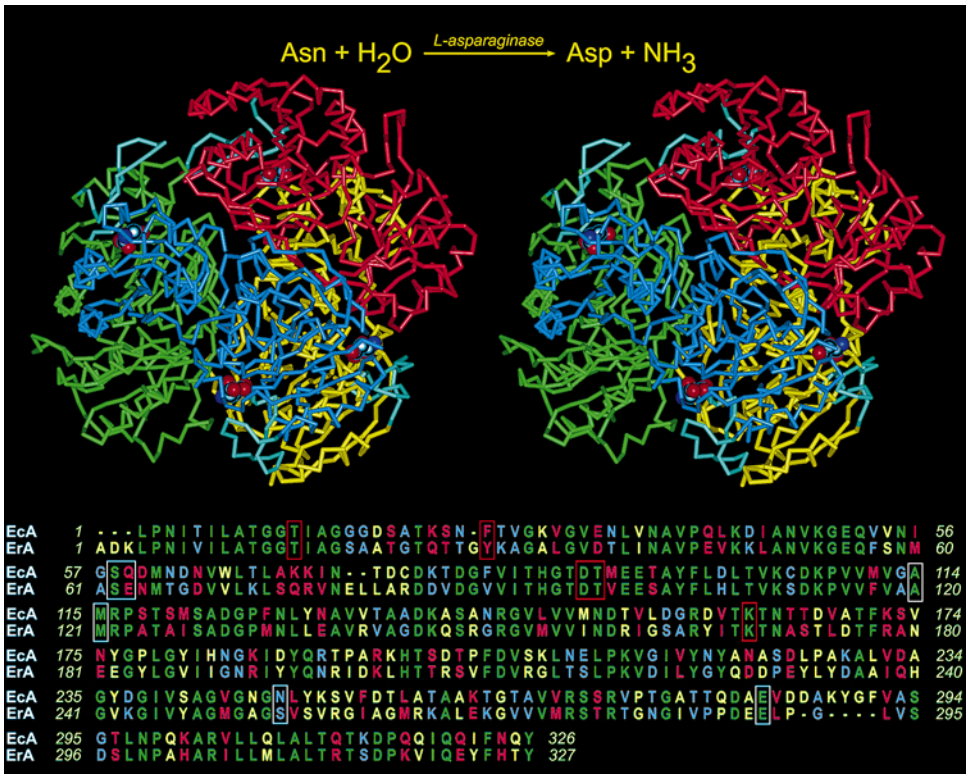


**Figure 1**
$C^{\alpha}$ trace of the Ec(Y25F) tetramer, with subunits marked in different colors (*A*, green; *B*, red; *C*, blue; *D*, yellow). The flexible loops shielding the active sites are colored cyan. The four active sites are marked by the molecules of L-aspartate (space-filling models), the product of the catalytic reaction. A general scheme for the catalytic reaction is shown at the top of the figure. Structure-based sequence alignment of the two asparaginases discussed in this paper is shown at the bottom, with identical residues highlighted in green and homologous residues in red. Residues forming the active site are outlined by boxes; those directly involved in the catalytic reaction are outlined by red boxes.

## 2. Materials and methods

### 2.1. EcA mutant Y25F

A sample of the Y25F mutant of EcA was a generous gift from Professor Klaus Röhm, Philipps Universität, Marburg, Germany. Initial crystallization conditions (citrate buffer pH 4.6, MPD precipitant, addition of $CaCl_2$) leading to the present hexagonal form of EcA were determined

**Table 1**
Crystal data and data collection and processing statistics for the hexagonal forms of bacterial L-asparaginases.

All diffraction images were processed using the *HKL* package (Otwinowski & Minor, 1997). Values in parentheses are for the last resolution shell.

| | | ErA | |
|---|---|---|---|
| | EcA (Y25F mutant) | Crystal S | Crystal L |
| Temperature (K) | 290 | 290 | 130 |
| Space group | $P6_522$ | $P6_122$ | $P6_122$ |
| Unit-cell parameters | | | |
| $a$ (Å) | 81.0 | 91.3 | 90.7 |
| $c$ (Å) | 341.1 | 346.3 | 339.4 |
| $V$ (Å$^3$) | 1937938 | 2498817 | 2419071 |
| $V_M$† (Å$^3$ Da$^{-1}$) | 2.34 | 2.97 | 2.87 |
| X-ray source | Synchrotron | Cu $K\alpha$ | Synchrotron |
| λ (Å) | 0.928 | 1.54178 | 0.928 |
| Detector | MAR Research 300 mm | R-AXIS II | MAR Research 300 mm |
| No. of reflections measured | 70502 | 89335 | 128226 |
| No. unique | 22309 | 29191 | 39022 |
| Resolution (Å) | 20–2.5 (2.59–2.50) | 20–2.4 (2.55–2.40) | 20–2.17 (2.25–2.17) |
| $R_{int}$ | 0.095 (0.362) | 0.105 (0.280) | 0.118 (0.373) |
| Average $I/\sigma(I)$ | 8.2 (2.0) | 10.0 (2.2) | 7.1 (2.0) |
| Completeness (%) | 92.5 (87.0) | 84.3 (66.8) | 86.8 (71.0) |

† Matthews volume (Matthews, 1968).

**Table 2**
Final models and refinement statistics for the hexagonal structures of bacterial L-asparaginases.

All refinements were performed in *CNS* (Brunger *et al.*, 1998).

| | | ErA | |
|---|---|---|---|
| | EcA (Y25F mutant) | Crystal S | Crystal L |
| Resolution (Å) | 10–2.5 | 10–2.4 | 10–2.17 |
| Reflections | | | |
| Criterion for observed | $F > 2\sigma(F)$ | $F > 2\sigma(F)$ | $F > 2\sigma(F)$ |
| Observed | 17776 | 27603 | 36655 |
| $R_{free}$ | 868 | 1371 | 1101 |
| Atoms | | | |
| Protein | 4860 | 4904 | 4706 |
| Water | 109 | 515 | 423 |
| Ligands | 18 | 10 | 10 |
| $R/R_{free}$ | 0.182/0.245 | 0.160/0.219 | 0.199/0.252 |
| Average $B$ factor (Å$^2$) | 47.30 | 20.35 | 22.03 |
| R.m.s. deviations from ideal | | | |
| Bonds (Å) | 0.009 | 0.008 | 0.010 |
| Angles (°) | 1.46 | 1.42 | 1.57 |
| Dihedrals (°) | 23.4 | 23.8 | 23.8 |
| Impropers (°) | 0.82 | 0.85 | 0.88 |
| Most favored $\varphi/\psi$ (%) | 84.2 | 87.2 | 89.4 |
| Additional allowed $\varphi/\psi$ (%) | 15.5 | 9.1 | 10.4 |
| PDB code | 1ho3 | 1hfj | 1hfk |

using the sparse-matrix method (Jancarik & Kim, 1991) and have been described in detail elsewhere (Kozak *et al.*, 2000). In addition to the Y25F form described herein, another variant of EcA, N248E, bearing a mutation in the C-terminal domain rather than in the N-terminal domain, has also been crystallized in this polymorphic modification (Kozak, 2000). Diffraction data for the Y25F mutant were collected at room temperature using synchrotron radiation (beamline X11, EMBL c/o DESY, Hamburg; Table 1). A significant increase in crystal mosaicity upon freezing prevented low-temperature data collection, but the crystals were stable enough at room temperature to allow complete data collection with only one crystal under such conditions. The structure was solved by molecular replacement using *AMoRe* (Navaza, 1994) and either the *AB* or *AD* dimer of native EcA (PDB code 3eca) as a molecular probe. Structure refinement was carried out in *CNS* (Brunger *et al.*, 1998) using the maximum-likelihood algorithm (Adams *et al.*, 1997) for the *AB* dimer with both active sites occupied by L-aspartate ligands. All structure factors with $F > 2\sigma(F)$ within the resolution range 10–2.5 Å were used and a global correction for bulk solvent was applied. Model stereochemistry was restrained using the parameters of Engh & Huber (1991) with slightly less restrictive weights than those suggested by *CNS*. Non-crystallographic symmetry (NCS) restraints (loose for side-chain atoms, more restrictive for main-chain atoms) were imposed on the two independent subunits (but not on their Asp ligands). Positional refinement alternated with *B*-factor refinement and with manual rebuilding and water verification (Jones & Kieldgaard, 1997). The progress of the refinement was monitored using $R_{free}$ (Brünger, 1992*a*) calculated for 868 (~5% of the total) randomly selected reflections (Table 2).

### 2.2. Two experimental studies of native ErA

A preparation of ErA was obtained as lyophilized powder from Program Resources Inc., Frederick, MD, USA and was used without further purification. As in the procedure described previously (Miller *et al.*, 1993), single crystals of ErA were grown from a protein solution of ~35 mg ml$^{-1}$ in 0.1 *M* CHES buffer pH 8.5 equilibrated against 47%(*w*/*v*) ammonium sulfate and 2%(*w*/*v*) PEG 400. In contrast to the standard vapor-diffusion method of equilibration, we allowed simultaneous concentration of the reservoir solution by evaporation in order to achieve much more rapid equilibration (Fig. 2). As a result, hexagonal crystals appeared in just 2–3 h after setting the sitting droplets and grew to final dimensions of 0.3 × 0.6 × 1.5 mm within an additional 10–12 h.

Some of the hexagonal crystals of ErA were stabilized by crosslinking in glutaraldehyde solution as described previously (Miller *et al.*, 1993), with subsequent gradual transfer to $(NH_4)_2SO_4$-free solution containing 30%(*w*/*v*) PEG 400 and 0.1 *M* L-hydroxylysine in 0.1 *M* acetate buffer pH 5.0. The intention of these experiments was to prepare crystalline complexes of ErA with L-hydroxylysine, a putative inhibitor of the enzyme, bound in the active site. However, the subsequent crystallographic studies proved these soaking experiments to be unsuccessful and we found that all crystals were essentially native. This result was confirmed by inhibition studies, in which no effect could be measured at concentrations of up to at least 50 m*M* L-hydroxylysine.

Two highly equivalent X-ray data sets were collected: one for untreated ErA crystals (S) and one for crystals soaked with L-hydroxylysine (L). Diffraction data for crystals S extending to 2.4 Å resolution were collected at room temperature using a conventional X-ray source, whereas those for crystals L were

collected at low temperature using synchrotron radiation (beamline X11, EMBL c/o DESY, Hamburg, Germany; 2.17 Å). The structure was solved from the synchrotron data using *X-PLOR* (Brünger, 1992*b*) and the *AC* dimer of 3eca as the molecular probe. Structure refinements for both data sets were carried out in *CNS* using the maximum-likelihood algorithm and all $F > 2\sigma(F)$ reflections after a global correction for bulk solvent. Protein stereochemistry was restrained according to Engh & Huber (1991), more and less tightly for models S and L, respectively. The two independent subunits were restrained by NCS in case S, but not in case L. Positional refinement alternated with *B*-factor refinement and with manual rebuilding and solvent interpretation (Jones & Kieldgaard, 1997). Residues 20–33, located in the flexible loops, were not included in model L because there was no interpretable electron density in those areas. The expected hydroxylysine ligand was not found in model L and eventually the active sites were interpreted to contain one sulfate anion each, similar to those of model S. In both cases, each step of model refinement/rebuilding was monitored through $R_{\rm free}$ calculations. The final models are of good quality (Table 2).

## 3. Results and discussion

### 3.1. New crystal forms of L-asparaginases

The initial aim of the studies reported here was to investigate some details of the catalytic mechanism of action of L-asparaginases by using mutations and by creating their complexes with putative inhibitors. The Y25F mutant of EcA was prepared in order to delineate the importance of the hydroxyl moiety of Tyr25 in catalysis. Although the mutated protein could be expressed and crystallized, the flexible loop that contained the modified residue was completely disordered and thus no structurally based conclusions about its role could be obtained. Similarly disappointing was the attempt to form a complex between ErA and L-hydroxylysine. The hydroxyl group of this putative ligand can be modeled to bind in the oxyanion hole (Lubkowski, Wlodawer, Ammon *et al.*, 1994) and we were interested in the structural details of such interactions. However, no electron density corresponding to the putative ligand could be observed in the active site. By contrast, a sulfate ion bound during crystallization could be identified there. The most important difference of the two ErA structures is that whereas in untreated crystals asparaginase has an active-site loop in the closed conformation, in the same crystals soaked in PEG 400 the loop has opened. Thus, although the primary aim of these studies was not realised, in the process of carrying them out we crystallized EcA and ErA in new hexagonal crystal forms which initially suggested isomorphism; however, the space groups were subsequently shown to be enantiomorphic.

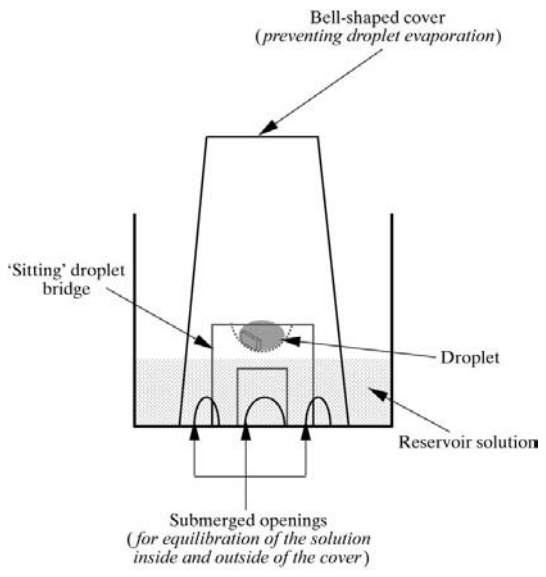


**Figure 2**
Diagram of the crystallization setup combining vapor diffusion and free evaporation of the reservoir solution.

### 3.2. Macromolecules crystallized in enantiomorphic space groups

The similarity of the crystallographic parameters for the hexagonal crystals of ErA and EcA initially suggested to us that the crystals of these two proteins were isomorphous. However, their actual space groups turned out to be enantiomorphic and this finding led us to investigate whether similar phenomena have been observed and reported in the past. The contents of the Protein Data Bank corresponding to the release of 20 October 1999 were scanned and the crystallographic parameters for all 2496 structures in the enantiomorphic space groups were written into a file. These coordinate sets were subsequently analyzed in order to remove multiple reports (such as mutants, ligand complexes *etc.*), resulting in the final set of 1013 structures. Many sets of unit-cell parameters were found to be similar purely by chance (404 enantiomorphic entries and 409 isomorphous pairs of entries within a 13% tolerance level), whereas the number of true enantiomorphs was very limited. We found only one pair of structures of virtually the same protein (native glyoxalase I and a form with two amino acids mutated) in enantiomorphic space groups $P4_1$ and $P4_3$ (Cameron *et al.*, 1999; Ridderstrom *et al.*, 1998). The quasi-isomorphous nature of those crystals was noted previously, but no further analysis of this phenomenon was provided (Ridderstrom *et al.*, 1998). Both crystal forms contain a tetramer (dimer of dimers) of glyoxalase I in the asymmetric unit and although the orientations of the tetramers in the respective asymmetric units are quite different, the residues involved in crystal contacts are surprisingly similar, with more than one-half of the contact residues being identical between the two crystal forms.

Additionally, we found two pairs of quasi-enantiomorphic structures of homologous enzymes from different sources, a situation analogous to the EcA–ErA pair. Two very highly homologous structures of bovine (Pearson *et al.*, 1998) and rat (Gupta *et al.*, 1999) ribonuclease A have been crystallized in the trigonal space groups $P3_121$ and $P3_221$, respectively, with similar unit-cell parameters. Although these two enzymes share 65% identity and an additional 15% similarity, the

crystal packing is completely different and practically none of the crystal contacts are made by equivalent residues. The other quasi-enantiomorphic pair involves citrate synthase from pig heart (Wiegand *et al.*, 1984) and from the hyperthermophilic archaeon *Pyrococcus furiosus* in the tetragonal space groups $P4_32_12$ and $P4_12_12$, respectively. These two enzymes share only 25% identity and their crystal contacts are completely different.

Finally, we found two structures of two complexes of DNA hexamers that were crystallized in the space groups $P4_32_12$ and $P4_12_12$ (Smith *et al.*, 1995; Dutta *et al.*, 1998). In the case of these oligonucleotides with very different sequences, the packing of the molecules is virtually the same despite the enantiomorphic nature of the unit cells.

### 3.3. Orientation of the ErA and EcA tetramers in the hexagonal unit cells

The crystal structures of L-asparaginases solved to date represent various realisations of the homotetramer 222 symmetry, ranging from cases in which only one subunit is independent and the tetrameric molecule is generated by crystallographic 222 symmetry (PGA; Lubkowski, Wlodawer, Ammon *et al.*, 1994) to cases, typified by the original EcA structure (Swain *et al.*, 1993), in which the symmetry of the tetramer is only approximate. The present structures provide interesting examples in this respect because only one twofold axis is perfect in each case and they represent different subunit relations. In the Y25F mutant of EcA, the crystallographic twofold axis generates the intimate *AC* dimer, whereas in ErA the intimate (*AC*) dimer is crystallographically independent and the twofold axis relates subunits that correspond to *AD* in the labeling system of 3eca. In both cases, the perfect twofold axis of the tetramer is aligned with the crystallographic $[1\bar{1}0]$ direction (see Fig. 3). The remaining (local) dyads are oriented differently with respect to the crystallographic symmetry directions, in particular relative to the *c* axis. To illustrate this orientation, the angles of these dyads with the (001) planes can be measured. In ErA, these angles are 81.9 and 8.1°, indicating approximate alignment with the principal hexagonal directions, whereas in EcA they are 52.8 and 37.2°. As a consequence of the different orientation of the non-crystallographic dyads in the crystals of the enzymes, the environment of the tetramer in each structure is also different (Fig. 3).

### 3.4. Tertiary and quaternary architectures: comparisons with previously reported structures

In only one of the previously published structures of L-asparaginases (AGA; Lubkowski, Wlodawer, Ammon *et al.*, 1994), the four monomers were related by three mutually perpendicular crystallographic dyads resulting in a tetramer with ideal $D_2$ symmetry. Such geometry also reflects the 'average' physiologically relevant form of L-asparaginases. In all other structures of these enzymes, however, this symmetry is not crystallographic. Nevertheless, in both examples presented in this report, the local twofold symmetry of the tetramers is nearly perfect. The degree of rotation of the axes generated for the $C^\alpha$ traces of various pairs of dimers using *ALIGN* (Cohen, 1997) deviates from 180° by less than 0.02°. This observation can also be represented in terms of the angular relations among the three dyads. In EcA, these angles deviate by less than 0.01° from 90°, whereas in ErA they are 90.00, 89.98 and 90.00°.

**Table 3**
Results of structural superpositions of monomers and their assemblies within and across different crystal structures of EcA and ErA (mon, monoclinic; hex, hexagonal).

The calculations, performed with *ALIGN* (Cohen, 1997), are illustrated by the numbers of superimposable $C^\alpha$ atom pairs and by the r.m.s. deviations between their positions.

| Molecules compared | | Average values† | |
|---|---|---|---|
| 1 | 2 | R.m.s. deviations (Å) | No. of Ca atoms |
| $EcA_{mon}$ monomer | $EcA_{mon}$ monomer | 0.22 | 310.7 |
| $EcA_{hex}$ monomer | $EcA_{hex}$ monomer | 0.04‡ | 320 |
| $EcA_{mon}$ monomer | $EcA_{hex}$ monomer | 0.32 | 302.8 |
| $EcA_{mon}$ dimer (*AB*) | $EcA_{mon}$ dimer (*AB*) | 0.41 | 606 |
| $ErA_{mon}$ monomer | $ErA_{mon}$ monomer | 0.16 | 315.5 |
| $ErA_{hex}$ monomer | $ErA_{hex}$ monomer | 0.05‡ | 321 |
| $ErA_{mon}$ monomer | $ErA_{hex}$ monomer | 0.16 | 316.1 |
| $ErA_{mon}$ dimer (*AB*) | $ErA_{hex}$ dimer (*AB*) | 0.17 | 631 |
| $EcA_{mon}$ monomer | $ErA_{mon}$ monomer | 0.76 | 301.7 |
| $EcA_{hex}$ dimer (*AB*) | $ErA_{hex}$ dimer (*AB*) | 0.85 | 601 |
| $EcA_{mon}$ tetramer | $EcA_{hex}$ tetramer | 0.41 | 1209 |
| $ErA_{mon}$ tetramer | $ErA_{hex}$ tetramer | 0.17 | 1252 |
| $EcA_{mon}$ tetramer | $ErA_{mon}$ tetramer | 0.90 | 1205 |
| $EcA_{hex}$ tetramer | $ErA_{hex}$ tetramer | 0.91 | 1206 |
| $EcA_{mon}$ tetramer | $ErA_{hex}$ tetramer | 0.89 | 1207 |
| $EcA_{hex}$ tetramer | $ErA_{mon}$ tetramer | 0.92 | 1206 |

† Whenever more than one superposition could be performed (*e.g.* six alignments of monomers are possible within a tetramer), the average values of r.m.s. deviation and number of aligned $C^\alpha$ atoms are shown. ‡ These unusually low values of r.m.s. deviations are the result of NCS restraints.

To assess the structural similarity of EcA and ErA, the monomers, dimers and tetramers of these enzymes were superimposed and r.m.s. deviations based on equivalent $C^\alpha$ atoms were calculated. The goals of the comparison were (i) to determine the structural conservation of monomers and dimers within one crystal form, (ii) to ascertain the effect of crystal packing on the structure of monomers, dimers and tetramers, and (iii) to compare structurally the $C^\alpha$ traces of EcA and ErA. Additionally, the results obtained from such comparisons were necessary for proper interpretation of the crystal contacts. The comparison included the monoclinic structures of EcA and ErA published previously (Swain *et al.*, 1993; Miller *et al.*, 1993) and the hexagonal structures [EcA(Y25F) and ErA(S)] presented in this report. The values of r.m.s. deviations are presented in Table 3. It is clear from these data that crystal packing does not affect the structure of the enzymes at any level (monomer, dimer or tetramer). More specifically, the monomers of EcA are structurally identical within 0.2–0.3 Å, whereas for ErA the equivalent r.m.s. deviations are even smaller. This difference may be attributed to the higher accuracy of the ErA structures. Because the r.m.s. deviations between the (*AB*) dimers as well as the tetramers taken from the monoclinic and hexagonal structures are 0.41 Å (EcA) and 0.17 Å (ErA) and are only marginally

higher than for the monomers, the quaternary structures of both proteins must also be independent of crystal packing. This structural conservation is especially pronounced for ErA, for which the r.m.s. deviation is virtually identical whenever monomers, dimers or tetramers are compared. The r.m.s. deviations of 0.76, 0.85 and 0.9 Å between monomers, dimers and tetramers, respectively, of EcA and ErA reflect the level of structural variability between these two proteins and also indicate that their quaternary structures are virtually identical. The latter conclusion indicates, for instance, that the tetramer of ErA can be reconstructed by four superpositions of the ErA monomer on each of the EcA monomers within the EcA tetramer. To test this hypothesis, we compared the tetramer of ErA taken from the monoclinic structure with a reconstructed ErA tetramer based on the EcA tetramer. The resulting r.m.s. deviation for 1307 $C^{\alpha}$ atoms is 0.51 Å.

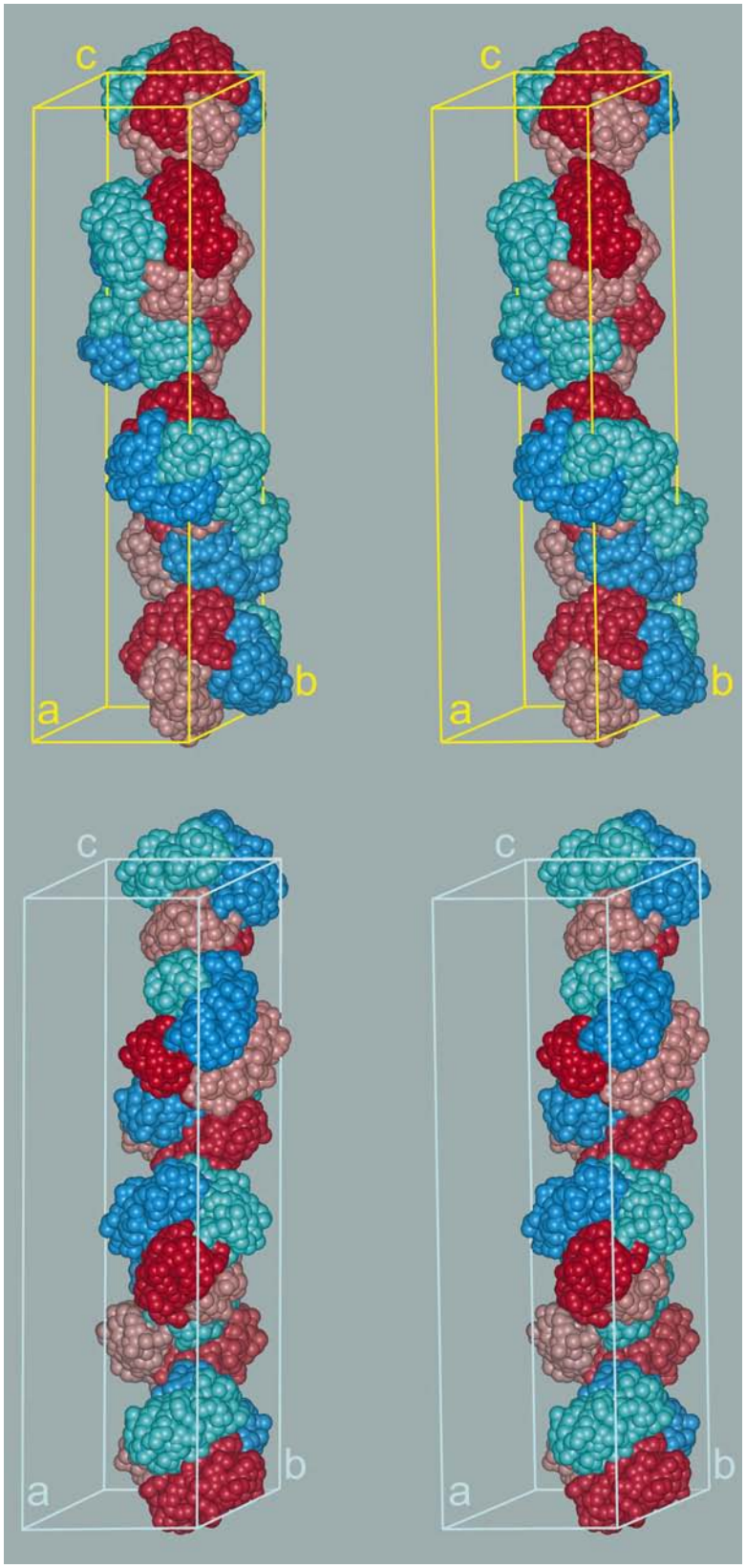


### 3.5. Analysis of crystal packing in the hexagonal crystals of asparaginases

The local environment of the tetramers is different in the structures of ErA and EcA (Fig. 3). The crystal packing difference between these two enantiomorphic structures is very clear when the arrangements of the tetramers along the sixfold axes are compared (Fig. 4). Variations in crystal packing are a direct consequence of the differences in the inter-tetramer contacts present in the crystals of both proteins. We have analyzed the crystal contacts in both EcA and ErA using the program *WHAT IF* (Vriend, 1990). An interatomic contact was detected when the distance between two atoms was smaller than of the sum of their van der Waals radii minus 0.25 Å. A complete list of crystal contacts was generated for both proteins, disregarding all interactions within the tetrameric molecules. These contacts mapped on the solvent-accessible surfaces of both proteins are shown in Fig. 5. A similar procedure was then repeated for two hypothetical crystals generated by tetramer reconstruction in the enantiomorphic space groups. One such crystal was generated by superposing ErA(S) monomers on the monomers in the EcA(Y25F) crystal lattice. In the second case, EcA(Y25F) monomers were placed in the ErA(S) lattice.

Based on the extensive structural and sequence similarity between EcA and ErA, we examined whether each of these enzymes could be crystallized

**Figure 3**
Stereoviews of the arrangement of the tetramers of EcA(Y25F) (upper panel) and ErA (lower panel) along the sixfold screw axes. The orientation of both lattices is the same. Only the $C^{\alpha}$ atoms (represented by the spheres) are shown, uniquely colored as in Fig. 1. The intimate dimers are formed by monomers *A* and *C* (green and blue) or *B* and *D* (red and yellow). The asymmetric unit of ErA consists of one intimate dimer. In the case of EcA, the asymmetric unit is formed by a looser dimer and the intimate dimers are formed across a crystallographic twofold axis.

with the packing and space group of its counterpart; that is, whether EcA could form $P6_122$ crystals and *vice versa*. The following modeling experiment was performed for this purpose. The ErA monomers were superimposed on the corresponding subunits of EcA in the crystal lattice of EcA and all inter-tetramer crystal contacts were analyzed. Analogously, in another experiment, the monomers of EcA replaced the monomers in the structure of ErA. Owing to the nearly perfect $D_2$ symmetry of both tetramers and their high structural similarity, no significant intratetramer steric violations were introduced by using individual monomers instead of complete tetramers in the superpositions. As seen in Fig. 6, for each protein several relatively well defined regions can be identified that are involved in unfavorable contacts when placed in the alternative unit cell. In neither case are clashes between symmetry-related molecules observed and only a few interatomic distances are significantly short. A closer analysis reveals, however, that some of these unfavorable interactions are the results of the unique features of each of the two enzymes. For example, a stretch of five residues (Ala287–Phe291) in the EcA molecule absent in ErA appears to be incompatible with the packing within the ErA lattice. Conversely, one of the shortest interactions found for the ErA model in the EcA unit cell involves Arg83, which substitutes for Cys77 in EcA. This cysteine residue forms the disulfide bond that is unique to the *E. coli* enzyme. Taking into account these observations, we consider it quite unlikely that either of these two enzymes could crystallize in the space group found for the other one with similar packing. The combined differences between many corresponding residues located on the surfaces of both enzymes not only contribute to the crystal packing differences but are also reflected more globally by different solvent contents, which in the two structures determined at room temperature are 47.4% for EcA(Y25F) and 58.6% for ErA(S).

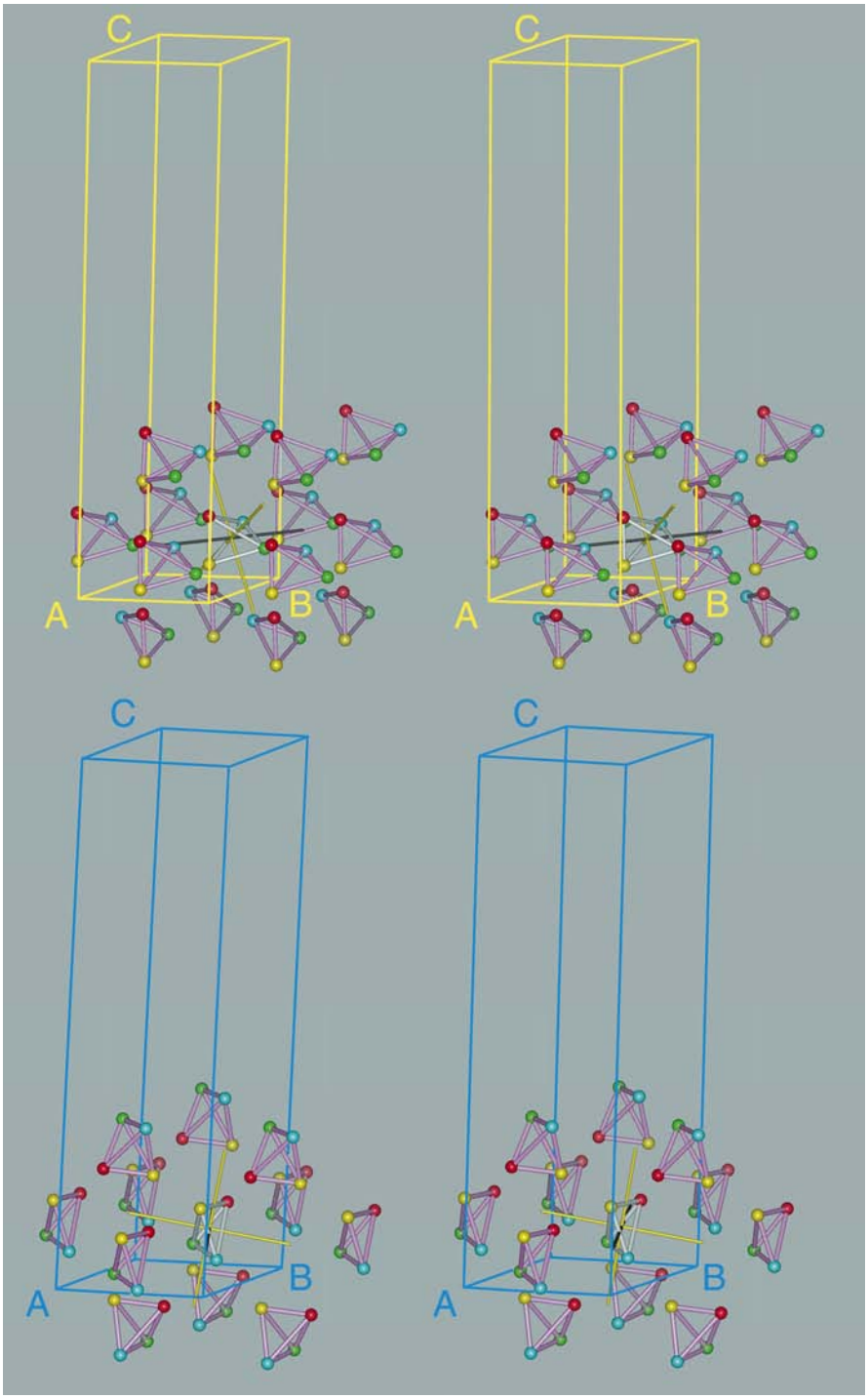


**Figure 4**
Stereoviews of the crystal packing of EcA (upper panel) and ErA (lower panel). The unit cells of both structures are viewed along the same direction. Each monomer is represented by a sphere, uniquely colored as in Fig. 1. Additionally, monomers within the biological tetramers are connected. Three molecular twofold axes, corresponding to the 222 symmetry, are shown for one (white) tetramer within each assembly. For each tetramer, one of the three twofold axes (black) relates two equivalent dimers. In both structures, this dyad axis coincides with the diagonal crystallographic twofold axis. Additionally, it can be seen that the arrangements of tetramers within both lattices are different.

## 4. Conclusions

A comparison of several structures of L-asparaginases shows that the loop acting as a gate over the active site (residues ~15–30) is very flexible. Its structure in the native enzyme is primarily controlled by the occupancy of the active site, *i.e.* by interactions between the ligand and the

loop residues, and only marginally by intermolecular interactions. In ErA the conformation of the active-site loop can be closed as in ErA(S) or open as in ErA(L), proving that in this crystal form the status of this loop is not determined by the crystal contacts. Generally, the loop is fixed in the closed conformation by the L-aspartate ligand in the active site. However, in the hexagonal EcA(Y25F) structure this is not the case. This finding indicates that the hydroxyl group of Tyr25 may be an important factor for loop stabilization. In ErA(S), with the sulfate anion occupying the position of the natural ligand (L-aspartate), the loop is found in closed orientation. In the presumably identical ErA(L) structure, the loop is not seen (and probably is not present in the closed conformation); the reason for this disparity can be attributed to the different treatment of the crystals prior to data collection. These examples indicate that the state of the flexible loop that covers the active site is sensitive to mutations and the presence of ligand molecules.

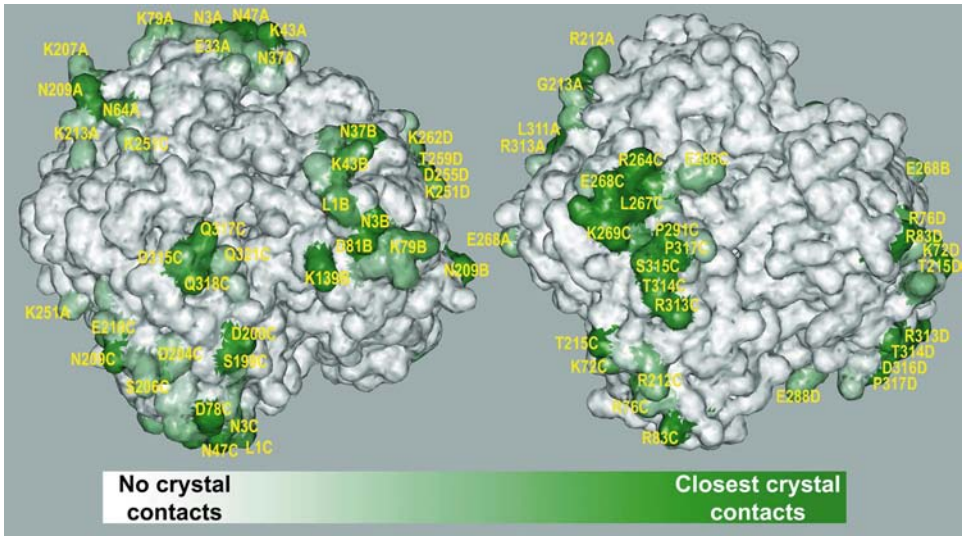


**Figure 5**
Crystal contacts mapped on the solvent-accessible surfaces of the EcA (left) and ErA (right) tetramers. In both tetramers, shown in identical orientation, only dimers are crystallographically unique. A list of crystal contacts that are shorter than 6.6 Å was generated using the program *WHAT IF* (Vriend, 1990). All intratetramer contacts were disregarded. Residues participating in crystal packing interactions are labeled.

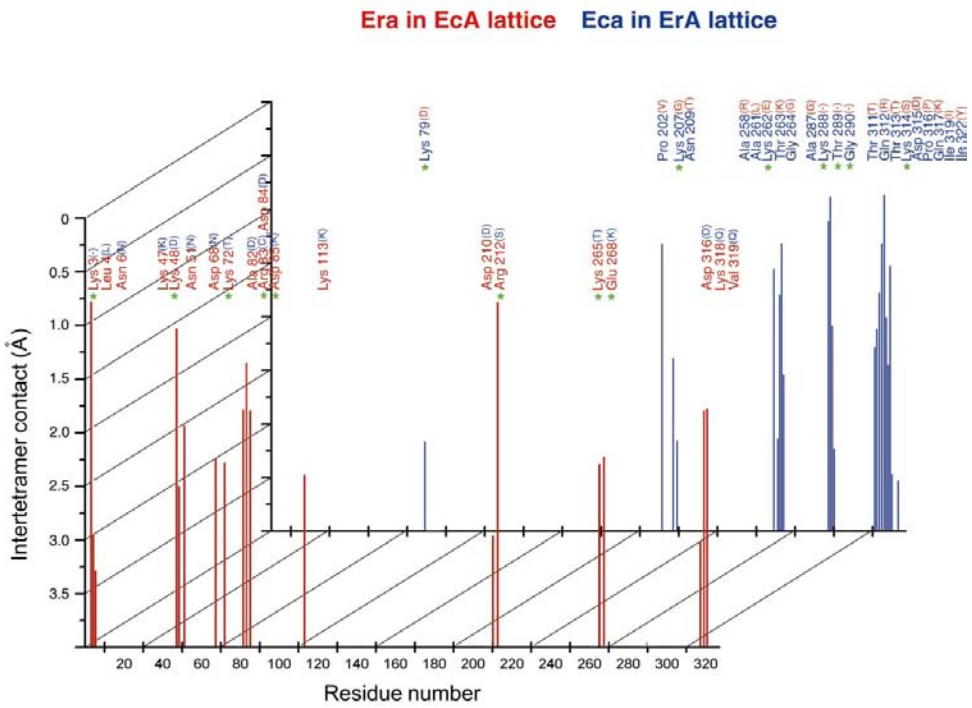


**Figure 6**
Crystal contacts of ErA(S) modeled in the EcA unit cell (red) and of EcA modeled in the ErA(S) unit cell (blue). Residues participating in a crystal contact are defined by type and number, followed by a one-letter code of the residue in the original protein (in parentheses). The most unfavorable contacts, related to differences in size and/or charge, are marked with green asterisks. See text for details.

The structures discussed here, together with previously published data, confirm the well known fact that protein crystal packing arrangements critically depend on very delicate and weak interactions. Consequently, multiple polymorphic forms of a protein and its variants can often be formed under virtually identical crystallization conditions (Lubkowski *et al.*, 1997). The numerous forms of EcA described to date are an excellent example. However, this does not mean that a given protein is compatible with any space-group symmetry, which is very well illustrated by EcA(Y25F) and ErA, where the small differences on the protein surface induce crystallization in space groups of opposite handedness and prevent isomorphism.

The analysis of the pseudo-enantiomorphic EcA–ErA pair leads us to conclude that the observed phenomenon is a complex mixture of different factors and currently not tractable in terms of definite rational models. A number of other observations, however, are also relevant. Superposition of either monomers or tetramers of L-asparaginase leads to virtually identical r.m.s. deviations, indicating that the tetramer archi-

tecture is the same in the two structures. By extension, this observation indicates that even when not required by space-group symmetry the L-asparaginase tetramers preserve nearly perfect 222 symmetry. All of these structures are very similar, with r.m.s. deviations at the monomer level of the order of 0.2 Å for pairs of ErA structures and 0.4 Å for pairs of EcA. Cross-superposition between ErA and EcA leads to a deviation of the order of 0.9 Å.

More generally, the examples of enantiomorphic crystals produced by closely related macromolecules discussed in this paper warrant a cautionary note. When searching for a new variant or a new modification of a macromolecular structure, one should carefully also consider those crystals that appear to represent the same crystallographic modification. The possibility should be investigated that the space group may be the mirror image of the old one and that the structure may in fact be very different.

We are grateful to Professor Klaus Röhm for his gift of the EcA mutant and to Anne Arthur for editorial comments. The research of Mariusz Jaskólski was supported in part by an International Research Scholar's award from the Howard Hughes Medical Institute. This project was also supported in part by North Atlantic Treaty Organization grant CRG940314 to Alexander Wlodawer. Beamline X11 at DESY was supported by HCMP Large Installations Project CHGE-CT93-0040.

## References

Adams, P. D., Pannu, N. S., Read, R. J. & Brünger, A. T. (1997). *Proc. Natl Acad. Sci. USA*, **94**, 5018–5023.
Beacham, I. & Jennings, M. (1990). *Today's Life Sci.* **2**, 40–42.
Bonthron, D. & Jaskólski, M. (1997). *Acta Biochim. Pol.* **44**, 491–504.
Brünger, A. T. (1992*a*). *Nature (London)*, **355**, 472–474.
Brünger, A. T. (1992*b*). *X-PLOR. Version 3.1. A System for X-ray Crystallography and NMR.* New Haven: Yale University Press.
Brunger, A. T., Adams, P. D., Clore, G. M., DeLano, W. L., Gros, P., Grosse-Kunstleve, R. W., Jiang, J. S., Kuszewski, J., Nilges, M., Pannu, N. S., Read, R. J., Rice, L. M., Simonson, T. & Warren, G. L. (1998). *Acta Cryst.* D**54**, 905–921.
Cameron, A. D., Ridderstrom, M., Olin, B., Kavarana, M. J., Creighton, D. J. & Mannervik, B. (1999). *Biochemistry*, **38**, 13480–13490.
Clavell, L. A., Gelber, R. D., Cohen, H. J., Hitchcock-Bryan, S., Cassady, J. R., Tarbell, N. J., Blattner, S. R., Tantravahi, R., Leavitt, P. & Sallan, S. E. (1986). *N. Engl. J. Med.* **315**, 657–663.
Cohen, G. E. (1997). *J. Appl. Cryst.* **30**, 1160–1161.
Derst, C., Henseling, J. & Röhm, K. H. (1992). *Protein Eng.* **5**, 785–789.
Derst, C., Wehner, A., Specht, V. & Röhm, K. H. (1994). *Eur. J. Biochem.* **224**, 533–540.
Dodson, G. & Wlodawer, A. (1998). *Trends Biochem. Sci.* **23**, 347–352.
Dutta, R., Gao, Y. G., Priebe, W. & Wang, A. H. (1998). *Nucleic Acids Res.* **26**, 3001–3005.
Engh, R. & Huber, R. (1991). *Acta Cryst.* A**47**, 392–400.
Gallagher, M. P., Marshall, R. D. & Wilson, R. (1989). *Essays Biochem.* **24**, 1–40.
Greenquist, A. C. & Wriston, J. C. Jr (1972). *Arch. Biochem. Biophys.* **152**, 280–286.
Gupta, V., Muyldermans, S., Wyns, L. & Salunke, D. M. (1999). *Proteins*, **35**, 1–12.
Harms, E., Wehner, A., Aung, H. P. & Röhm, K. H. (1991). *FEBS Lett.* **285**, 55–58.
Hill, J. M., Roberts, J., Loeb, E., Khan, A., MacLellan, A. & Hill, R. W. (1967). *J. Am. Med. Assoc.* **202**, 882–888.
Jakob, C. G., Lewinski, K., LaCount, M. W., Roberts, J. & Lebioda, L. (1997). *Biochemistry*, **36**, 923–931.
Jancarik, J. & Kim, S.-H. (1991). *J. Appl. Cryst.* **24**, 409–411.
Jones, T. A. & Kieldgaard, M. (1997). *Methods Enzymol.* **277**, 173–208.
Kozak, M. (2000). PhD thesis, A. Mickiewicz University, Poznan, Poland.
Kozak, M., Jasólski, M. & Röhm, K. H. (2000). *Acta Biochim. Pol.* **47**, 807–814.
Lubkowski, J., Bujacz, G., Boque, L., Domaille, P. J., Handel, T. M. & Wlodawer, A. (1997). *Nature Struct. Biol.* **4**, 64–69.
Lubkowski, J., Palm, G. J., Gilliland, G. L., Derst, C., Röhm, K. H. & Wlodawer, A. (1996). *Eur. J. Biochem.* **241**, 201–207.
Lubkowski, J., Wlodawer, A., Ammon, H. L., Copeland, T. D. & Swain, A. L. (1994). *Biochemistry*, **33**, 10257–10265.
Lubkowski, J., Wlodawer, A., Housset, D., Weber, I. T., Ammon, H. L., Murphy, K. C. & Swain, A. L. (1994). *Acta Cryst.* D**50**, 826–832.
Matthews, B. W. (1968). *J. Mol. Biol.* **33**, 491–497.
Miller, M., Rao, J. K. M., Wlodawer, A. & Gribskov, M. R. (1993). *FEBS Lett.* **328**, 275–279.
Navaza, J. (1994). *Acta Cryst.* A**50**, 157–163.
Ortlund, E., LaCount, M. W., Lewinski, K. & Lebioda, L. (2000). *Biochemistry*, **39**, 1199–1204.
Otwinowski, Z. & Minor, W. (1997). *Methods Enzymol.* **276**, 307–326.
Palm, G. J., Lubkowski, J., Derst, C., Schleper, S., Röhm, K. H. & Wlodawer, A. (1996). *FEBS Lett.* **390**, 211–216.
Pearson, M. A., Karplus, P. A., Dodge, R. W., Laity, J. H. & Scheraga, H. A. (1998). *Protein Sci.* **7**, 1255–1258.
Ridderstrom, M., Cameron, A. D., Jones, T. A. & Mannervik, B. (1998). *J. Biol. Chem.* **273**, 21623–21628.
Smith, C. K., Davies, G. J., Dodson, E. J. & Moore, M. H. (1995). *Biochemistry*, **34**, 415–425.
Swain, A. L., Jaskólski, M., Housset, D., Rao, J. K. M. & Wlodawer, A. (1993). *Proc. Natl Acad. Sci. USA*, **90**, 1474–1478.
Vriend, G. (1990). *J. Mol. Graph.* **8**, 52–56.
Wehner, A., Harms, E., Jennings, M. P., Beacham, I. R., Derst, C., Bast, P. & Röhm, K. H. (1992). *Eur. J. Biochem.* **208**, 475–480.
Wiegand, G., Remington, S., Deisenhofer, J. & Huber, R. (1984). *J. Mol. Biol.* **174**, 205–219.